Strong tensor forces and the possibility of high-spin states in the nucleon-antinucleon system

C. B. Dover
Brookhaven National Laboratory, Upton, N. Y. 11973

J. M. Richard*
Department of Physics, State University of New York, Stony Brook, N. Y. 11794
(Received 2 May 1977)

The antinucleon-nucleon ($\bar{N}N$) potential, in isospin $I = 0$ states, contains a strong tensor component which is a *coherent* sum of contributions from different meson exchanges. The large mixing of $L = J - 1$ and $L = J + 1$ orbital momenta induced by the tensor potential can produce $I = 0$ high-spin states ($3^-, 4^+, 5^-$) relatively near to the $\bar{N}N$ threshold.

I. INTRODUCTION

There has been renewed interest recently in the theoretical study of low-energy antinucleon-nucleon ($\bar{N}N$) interactions, in particular in the spectrum of bound states and resonances close to threshold.[1-5] The principal motivation for this activity is the recent experimental evidence for structure in the low-energy $\bar{N}N$ cross section.[6-8] It is possible that certain heavy mesons near the $\bar{N}N$ threshold could, in a bootstrap or quark-model scheme, contain a sizable proportion of the $\bar{N}N$ configuration. Other alternatives have also been recently advanced.[9, 10]

Independent of these considerations, the $\bar{N}N$ interaction near threshold is doubly interesting from the theoretical point of view, since the potential of long and medium range also enters into the study of nuclear forces (NN), while the understanding of the mechanisms of annihilation is intimately connected to the study of hadronic reactions at high energy.

Several authors have included absorptive effects in the $\bar{N}N$ scattering or bound-state problem.[11, 12] They use an absorptive local potential $W(r)$ or a boundary condition model. In this picture, most of the bound states and resonances of the real potential acquire a large width. The problem of widths has also been considered in a recent paper by Shapiro,[13] who argues that such states will *not* be greatly shifted or broadened by annihilation processes. In this work, we provisionally adopt this viewpoint[13] and limit ourselves to a study of the real part of the interaction.

In this context, the purpose of this article is to examine in more detail the role of tensor forces in the isospin $I = 0$ states. This component was included in most of the previous estimates of $\bar{N}N$ cross sections via potential models, but was omitted completely[1] or partially[4] in some previous work on the $\bar{N}N$ bound-state spectrum. In other recent work,[5] where both the diagonal and nondiagonal tensor potentials were included, the high-spin states ($J > 2$) were not studied. We show here that the correct inclusion of the tensor component clarifies the nature of the $\bar{N}N$ spectrum in natural-parity states. We see that a strong tensor potential can cause $I = 0$ high-spin states to lie at relatively low energies, but no corresponding $I = 1$ high-spin ($J \geq 3$) states are expected in the $\bar{N}N$ model.

II. SOME PROPERTIES OF THE MEDIUM- AND LONG-RANGE PART OF THE $\bar{N}N$ POTENTIAL

In this article, we describe the $\bar{N}N$ interaction by a nonrelativistic potential. Of course, for deeply bound states, relativistic corrections could be important, but here we are less interested in the precise absolute value of binding energies than in the relative *ordering* of levels and the change in binding obtained for a given level when the spin-dependent parts of the force (tensor forces in particular) are included. The Schrödinger-equation framework seems sufficient for these purposes.

The part of the $\bar{N}N$ potential of medium and long range is mediated by the exchange of mesons and can be deduced from the corresponding NN potential by the G-parity rule, which states that contributions of mesons of odd G parity change sign. This induces important qualitative modifications of the interaction. For example, the ω exchange, which is repulsive for NN systems, becomes attractive for $\bar{N}N$ and adds coherently to the attractive potential due to the exchange of two pions in an $I = 0$ S state (ϵ exchange in one boson models). The central potential $V_C^+(r)$ is thus deeper for $\bar{N}N$ than for NN.

Important changes appear also in the spin-dependent part of the potential. In the NN case, the most clear coherence appears in the $I = 1$ spin-orbit potential (see Table I and Fig. 1). This co-

TABLE I. Signs of meson-exchange contributions to Wigner (V_C), spin-spin (V_{SS}), spin-orbit (V_{LS}), and tensor (V_T) potentials for the NN system.

	$I=0$				$I=1$			
Meson	V_C	V_{SS}	V_{LS}	V_T	V_C	V_{SS}	V_{LS}	V_T
π	0	−	0	−	0	+	0	+
η	0	+	0	+	0	+	0	+
ρ	−	−	+	+	+	+	−	−
ω	+	+	−	−	+	+	−	−
δ	+	0	+	0	−	0	−	0
ϵ	−	0	−	0	−	0	−	0

herence allows one to largely explain the observed difference between the $^3P_0$, $^3P_1$, and $^3P_2$ proton-proton phase shifts. Tensor forces in the NN case play a secondary role in $I=1$ states, but a more important role for $I=0$ states. For example, the mixing angles[14] $\bar{\epsilon}_1$ and $\bar{\epsilon}_3$ are larger than $\bar{\epsilon}_2$ and $\bar{\epsilon}_4$; the effect is even more marked if one utilizes eigenphaseshifts[15] instead of nuclear-bar phase shifts.[14] This difference between $I=1$ and $I=0$ tensor potentials arises because, in the latter case, the ω and π exchange contributions have the same sign. The coherence is limited, however, by a ρ exchange contribution of the opposite sign

TABLE II. Signs of contributions to V_C, V_{SS}, V_{LS}, V_T for the $\bar{N}N$ system.

	$I=0$				$I=1$			
Meson	V_C	V_{SS}	V_{LS}	V_T	V_C	V_{SS}	V_{LS}	V_T
π	0	+	0	+	0	−	0	−
η	0	+	0	+	0	+	0	+
ρ	−	−	+	+	+	+	−	−
ω	−	−	+	+	−	−	+	+
δ	−	0	−	0	+	0	+	0
ϵ	−	0	−	0	−	0	−	0

(see Table I).

In the case of the $\bar{N}N$ interaction, all meson exchanges give a contribution of the same sign to the $I=0$ tensor potential (see Table II). This tensor coherence is a general feature of all such meson exchange models, although its strength depends on the choice of coupling constants. It occurs whether one uses a pole approximation for ρ and ϵ exchange or a more rigorous and complete treatment of two-pion exchange based on dispersion relations.[5,16] For example, in Fig. 2 we display the theoretical part ($\pi+2\pi+\omega$ exchange) of the NN and $\bar{N}N$ tensor potentials, as per Ref. 5, for both $I=0$ and 1. We

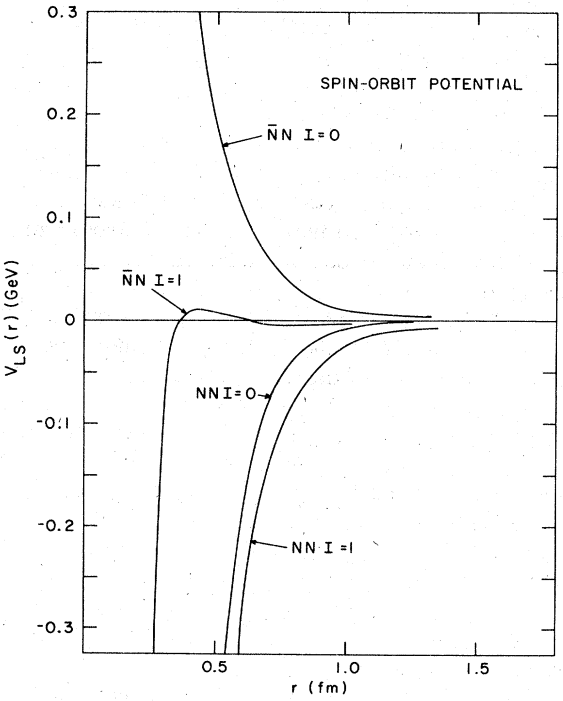

FIG. 1. The spin-orbit potential $V_{LS}(r)$ as a function of r for the $I=0$ and 1 states of the NN and $\bar{N}N$ systems. The curves are obtained from the Paris potential of Ref. 5. The dominance of the $I=1$ NN channel is due to the coherence of vector and scalar meson contributions to $V_{LS}(r)$.

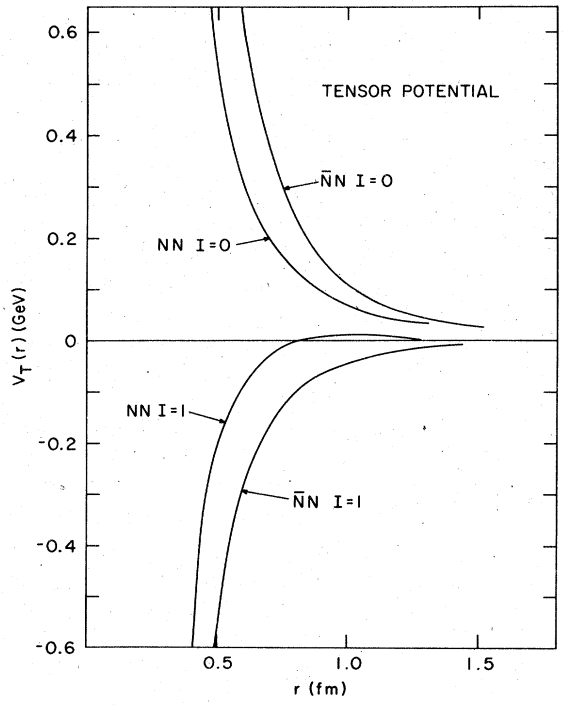

FIG. 2. The tensor potential $V_T(r)$ for the NN and $\bar{N}N$ systems in $I=0$ and 1 states. The curves correspond to the model of Ref. 5. The coherence of pseudoscalar and vector contributions leads to the largest values of $V_T(r)$ in the $I=0$ $\bar{N}N$ channel. The curve for NN $I=0$ has been multiplied by −1.

see that the $\bar{N}N$ $I=0$ tensor potential is by far the most important.

III. EFFECT OF THE TENSOR FORCES IN THE $\bar{N}N$ SYSTEM

For natural-parity states ($L=J\pm1$), the tensor potential leads to coupled radial equations. In the $\{LSJ\}$ representation, they are governed by the potentials

$$V_{11}(r)=V_C(r)+V_{SS}(r)+(J-1)V_{LS}(r)-\frac{2(J-1)}{2J+1}V_T(r)+(J-1)^2V_{LS2}(r)+\frac{\hbar^2}{M}\frac{J(J-1)}{r^2},$$

$$V_{22}(r)=V_C(r)+V_{SS}(r)-(J+2)V_{LS}(r)-\frac{2(J+2)}{2J+1}V_T(r)+(J+2)^2V_{LS2}(r)+\frac{\hbar^2}{M}\frac{(J+1)(J+2)}{r^2}, \tag{3.1}$$

$$V_{12}(r)=6[J(J+1)]^{1/2}V_T(r)/(2J+1),$$

in terms of the usual central (V_C), spin-spin (V_{SS}), spin-orbit (V_{LS}), tensor (V_T), and quadratic spin-orbit (V_{LS2}) components.

In some of the previous work[1] on the $\bar{N}N$ system, tensor forces were completely neglected. This approximation is not at all justified.[4] In some later work,[4] only the diagonal matrix elements of the tensor potential were included. This approximation is adequate for $I=1$ states but qualitatively wrong for $I=0$ states, where it leads to a moderate amount of attraction in *both* the $^{2J+1,2S+1}L_J = {}^{13}(J-1)_J$ and $^{13}(J+1)_J$ channels. In fact, the orbital part of the $I=0$ eigenfunctions are close to one of the configurations $|\alpha_J\rangle$ or $|\beta_J\rangle$ which diagonalize the tensor-force operator:

$$|\alpha_J\rangle=[(J+1)^{1/2}|L=J-1\rangle+J^{1/2}|L=J+1\rangle]/(2J+1)^{1/2},$$
$$|\beta_J\rangle=[-J^{1/2}|L=J-1\rangle+(J+1)^{1/2}|L=J+1\rangle]/(2J+1)^{1/2}. \tag{3.2}$$

In this basis, the potential has the form

$$V_{\alpha\alpha}(r)=V_C(r)+V_{SS}(r)-V_{LS}(r)+2V_T(r)+(J^2+J+1)V_{LS2}(r)+\frac{\hbar^2}{M}\frac{J(J+1)}{r^2},$$

$$V_{\beta\beta}(r)=V_C(r)+V_{SS}(r)-2V_{LS}(r)-4V_T(r)+(J^2+J+4)V_{LS2}(r)+\frac{\hbar^2}{M}\frac{J^2+J+2}{r^2}, \tag{3.3}$$

$$V_{\alpha\beta}(r)=[J(J+1)]^{1/2}[-V_{LS}(r)+3V_{LS2}(r)+2\hbar^2/Mr^2].$$

One sees from Eq. (3.3) that the effective tensor force is *repulsive* in channel α for $I=0$ and strongly *attractive* in channel β in this new representation.

For $\bar{N}N$ bound states, one can utilize Eq. (3.3) without difficulty to calculate the spectrum. We will also employ a new approximation, which consists of neglecting the coupling $V_{\alpha\beta}$; in this case, the corresponding states are the eigenfunctions of the tensor operator Ω_T. The validity of this approximation is a measure of the dominance of tensor forces over spin-orbit and centrifugal effects which tend to mix eigenstates of Ω_T.

IV. RESULTS

For the numerical calculations, we have considered two different models: (a) the one-boson-exchange model of Bryan and Phillips,[12] and (b) the Paris potential of Ref. 5, which contains pion and ω exchange, supplemented by a two-pion exchange contribution evaluated from dispersion relations.

The spectra of unnatural-parity states arising from these potentials can be found in Refs. 4 and 5. For the Bryan and Phillips potential, Ref. 4 includes only diagonal tensor forces in the natural-parity $L=J\pm1$ states. For the Paris potential, the full tensor component was included in Ref. 5, but the results for $I=0$ were given only for $J\leq2$.

For $I=0$ natural-parity bound states (calculated here without any absorptive potential), we have compared the results obtained with different prescriptions for handling the spin-dependent forces:

(i) without the tensor potential ($V_T=0$),

(ii) including only the diagonal part of the potential in the $\{L,S,J\}$ representation ($V_{12}=0$),

(iii) neglecting the off-diagonal coupling terms in Eq. (3.3), i.e., $V_{\alpha\beta}=0$,

(iv) including all diagonal and off-diagonal components of the potential.

For the calculation of the energies of $I=0$ resonances, we are limited to cases (i), (ii), and (iv). The $I=1$ states are obtained with prescription (iv); i.e., with the complete potential. The G-parity transformation is only used to generate the $\bar{N}N$ potential for $r\geq r_0$. For the Bryan-Phillips potential, we set $V(r)=0$ for $r\leq r_0$, using the same value $r_0=0.6$ fm as for the NN problem.[16] For the Paris potential,[5] we set $V(r)=V(r_0)$ for $r\leq r_0$, i.e., we assume a square well at short distances. A value $r_0=0.75$ fm was chosen in order to position the low-spin $I=0$ bound states (0^+, 1^-, 2^+) *above* the corresponding physical mesons (ϵ, ω, f), which are presumably composed mostly of $\bar{q}q$ configurations in the quark model. Of course, our choice of short-range cutoff is necessarily rather arbitrary. It was shown pre-

TABLE III. Binding energies (in MeV) of natural-parity $\bar{N}N$ bound states and resonances for the Bryan-Phillips[12] potential with $r_0 = 0.6$ fm. For approximation (iii), only bound states are given; β_1^* denotes a bound radial excitation ($n = 1$) of type β_1; only the exact results are given for $I = 1$ states.

State	Approx. (i) ($V_T = 0$)	Approx. (ii) ($V_{12} = 0$)	Approx. (iii) ($V_{\alpha\beta} = 0$)	Exact (iv)
$^{13}P_0$	−629	$<-2M$ ($n = 0$); −68 ($n = 1$)	same as (ii)	same as (ii)
$^{13}S_1$-$^{13}D_1$	−484 ($^{13}S_1$); −471 ($^{13}D_1$)	−484 ($^{13}S_1$); −1119 ($^{13}D_1$)	−1783 (β_1); −13 (β_1^*)	−1791 ($n = 0$); −42 ($n = 1$); +7 ($n = 1$)
$^{13}P_2$-$^{13}F_2$	−71 ($^{13}P_2$); −182 ($^{13}F_2$)	−264 ($^{13}P_2$); −687 ($^{13}F_2$)	−1435 (β_2)	−1452 ($n = 0$); +302 ($n = 1$)
$^{13}D_3$-$^{13}G_3$	+180 ($^{13}D_3$); +215 ($^{13}G_3$)	+50 ($^{13}D_3$); −200 ($^{13}G_3$)	−935 (β_3)	−962
$^{13}F_4$-$^{13}H_4$	+715 ($^{13}H_4$)	+370 ($^{13}H_4$)	−311 (β_4)	−348
$^{13}G_5$-$^{13}I_5$	...	...	...	+330
$^{33}P_0$				+23
$^{33}S_1$-$^{33}D_1$				−143
$^{33}P_2$-$^{33}F_2$				+17

viously[5] that while the absolute values of binding energies are very sensitive to a change of the cut-off radius, the level order is very stable.

The results of calculations using approximations (i)–(iv) are shown in Tables III–VI. An examination of these results leads to the following observations: For $I = 0$ states, the complete neglect of tensor forces (i) is a very bad approximation; it leads to qualitative changes in the spectrum. Neglecting the off-diagonal coupling V_{12} in Eq. (3.1) [approximation (ii)] is also poor for $I = 0$ natural-parity states. On the other hand, the neglect of the off-diagonal coupling $V_{\alpha\beta}$ in representation (3.2) is a very good approximation (iii) for the same states.

For small $J(\leq 2)$, it appears that the approximation $V_{12} = 0$ in Eq. (3.1) generally leads to *two* bound states $^{13}(J-1)_J$ and $^{13}(J+1)_J$ having the *same* external quantum numbers. On the contrary,

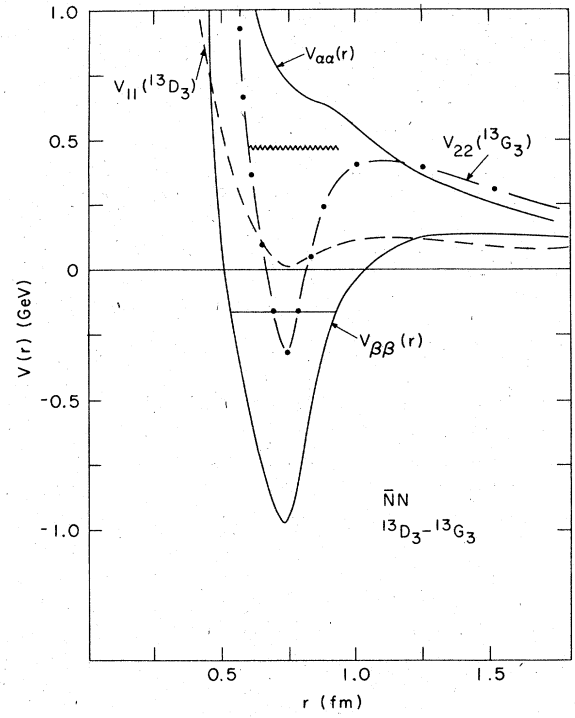

FIG. 3. Effect of nondiagonal tensor forces on the $I = 0$, $J^P = 3^-$ states. The potentials $V_{11}(r)$ and $V_{22}(r)$ of Eq. (3.1) for the $^{13}D_3$ and $^{13}G_3$ channels are plotted as dashed and dot-dashed curves, respectively; these include only the *diagonal* part of the tensor potential. $V_{22}(r)$ produces a wide resonance, at an energy indicated by the wavy line. The potentials $V_{\alpha\alpha}(r)$ and $V_{\beta\beta}(r)$, corresponding to the representation of Eq. (3.2) are shown as solid curves; $V_{\beta\beta}(r)$ produces a bound state shown as a solid line. The downward energy shift due to the *off-diagonal* tensor coupling is about 600 MeV. Calculations were done with the potential of Ref. 5.

TABLE IV. Wave-function admixtures for $\bar{N}N$ bound states in the $\{LSJ\}$ and $\{\alpha_J, \beta_J\}$ representations. These wave functions correspond to the exact values (iv) of Table III, using the Bryan-Phillips[12] potential with $r_0 = 0.6$ fm.

State	% of $L = J-1$	% of $L = J+1$	% of α_J	% of β_J
$^{13}S_1$-$^{13}D_1$ $(n=0)$	32	68	0.2	99.8
$^{13}S_1$-$^{13}D_1$ $(n=1)$	82	18	42	58
$^{13}P_2$-$^{13}F_2$	37	63	0.3	99.7
$^{13}D_3$-$^{13}G_3$	38	62	0.5	99.5
$^{13}F_4$-$^{13}H_4$	40	60	0.8	99.2
$^{13}S_1$-$^{33}D_1$	97	3	81	19

the complete calculation yields only *one* deeply bound state (in some cases with a bound radial excitation) corresponding to the fully coherent mixture $|\beta_J\rangle$ of the two different L values. The other configuration $|\alpha_J\rangle$ of Eq. (3.2) does not generally correspond to a bound state, since the effective tensor potential is repulsive. The complete calculation thus yields a spectrum which is considerably simplified.

For larger values of J (>2), the effect of tensor forces has also been underestimated in previous work.[1,4] For example, for the coupled states $^{13}F_4 - {}^{13}H_4$, we have $\langle {}^3F_4|\Omega_T|{}^3F_4\rangle = -\frac{2}{3}$ and $\langle {}^3H_4|\Omega_T|{}^3H_4\rangle = -\frac{4}{3}$. However, we find that the wave function for the 4^+ resonance is very close to $|\beta_4\rangle$, for which $\langle\beta_4|\Omega_T|\beta_4\rangle = -4$. This strong mixing of L values will occur for any model with strong tensor forces. The coherence of tensor forces in the main dynamical mechanism which can allow certain selected $\bar{N}N$ configurations *up to high spin* ($I=0, J^{PC} = 0^{++}$, 1^{--}, 2^{++}, 3^{--}, 4^{++}, 5^{--}) to be bound or resonate at low energies.

The wave-function admixtures for $\bar{N}N$ states are shown in Tables IV and VI for the $\{LSJ\}$ and $\{\alpha_J, \beta_J\}$ representations of Eqs. (3.1) and (3.2), respectively. The results for the Bryan-Phillips potential (Table IV) and the Paris potential (Table VI) are very similar. For each $n=0$ state of the natural-parity band (1^-, 2^+, 3^-, etc.), the wave functions are close to the fully coherent admixture $|\beta_J>$ of $L = J \pm 1$ components given by Eq. (3.2). In the $|\alpha_J\rangle$, $|\beta_J\rangle$ basis, the wave functions are found to consist of almost 100% of configuration $|\beta_J\rangle$, with only small admixtures of $|\alpha_J\rangle$. Approximation (iii), which neglects this admixture, is thus a very good approximation both for the energies and wave functions of the $I=0$ natural-parity band. The coherent tensor coupling for $I=0$ completely dominates the centrifugal and spin-orbit contributions, which tend to mix $|\alpha_J\rangle$ and $|\beta_J\rangle$. For $I=0$ radial excitations ($n=1$) and natural-parity $I=1$ states, on the other hand, the situation is more reminiscent of the deuteron, with only a small $^3D_1$ admixture to a dominant $^3S_1$ configuration. In this case, the usual $\{LSJ\}$ basis is more appropriate than $|\alpha_J\rangle$ and $|\beta_J\rangle$. For $I=1$ states, there is no overall coherence of tensor forces, and the net tensor strength is of the same

TABLE V. Binding energies (in MeV) of natural-parity $\bar{N}N$ bound states and resonances for the Paris potential[5] with a cutoff of 0.75 fm. For $I=1$ states, only the complete calculation is given; only bound states are listed for approximation (iii).

State	Approx. (i) $(V_T = 0)$	Approx. (ii) $(V_{12} = 0)$	Approx. (iii) $(V_{\alpha\beta} = 0)$	Exact (iv)
$^{13}P_0$	...	−888 $(n=0)$; −31 $(n=1)$	same as (ii)	same as (ii)
$^{13}S_1$-$^{13}D_1$	−37 ($^{13}S_1$)	−37 ($^{13}S_1$); −175 ($^{13}D_1$)	−711 (β_1)	−751 $(n=0)$; −3 $(n=1)$
$^{13}P_2$-$^{13}F_2$	+565 ($^{13}F_2$)	−130 ($^{13}F_2$)	−443 (β_2)	−477
$^{13}D_3$-$^{13}G_3$	...	+460 ($^{13}G_3$)	−126 (β_3)	−159
$^{13}F_4$-$^{13}H_4$	...	...	...	+162
$^{13}G_5$-$^{13}I_5$	...	...	...	+552
$^{33}S_1$-$^{33}D_1$				−137

TABLE VI. Wave-function admixtures for $\bar{N}N$ bound states in the $\{LSJ\}$ and $\{\alpha_J, \beta_J\}$ representations. These wave functions correspond to the exact results (iv) of Table V, using the Paris potential[5] with $r_c = 0.75$ fm.

State	% of $L = J-1$	% of $L = J+1$	% of α_J	% of β_J
$^{13}S_1$-$^{13}D_1$ $(n=0)$	44	56	2	98
$^{13}S_1$-$^{13}D_1$ $(n=1)$	75	25	21	79
$^{13}P_2$-$^{13}F_2$	52	48	2	98
$^{13}D_3$-$^{13}G_3$	58	42	3	97
$^{33}S_1$-$^{33}D_1$	94	6	87	13

order as the centrifugal and spin-orbit contributions.

The total potentials $V(r)$ for the uncoupled $^{13}D_3$ and $^{13}G_3$ configurations [V_{11} and V_{22} of Eq. (3.1)] are shown in Fig. 3, along with the diagonal potentials $V_{\beta\beta}(r)$ and $V_{\alpha\alpha}(r)$ for the coupled $^{13}D_3$-$^{13}G_3$ system in Eq. (3.3). The effect of the off-diagonal tensor coupling is seen to be an appreciable deepening of the attractive well in channel $|\beta\rangle$; the potential is strongly *repulsive* in channel $|\alpha\rangle$. The effect of the off-diagonal coupling is to produce a large shift in the binding energy; the shift is 600 MeV for the 3^- state shown in Fig. 3, and comparable amounts for other spins.

The diagonal (and dominant) potential $V_{\beta\beta}(r)$ is shown in Fig. 4 for the 3^- member of the $I=0$ natural-parity band. The square of the radial wave function $b_J(r)$ is also shown. The wave function is sharply localized in the attractive pocket of the potential around 0.75 fm. For each state of the natural-parity band, the rms radius exceeds 0.75 fm and increases somewhat with J for these models.

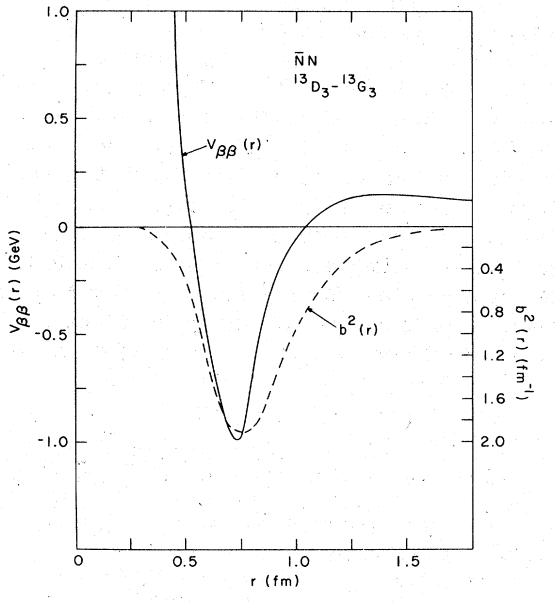

FIG. 4. The diagonal potential $V_{\beta\beta}(r)$ of Eq. (3.3) is plotted as a solid curve for the 3^- member of the $I=0$ natural-parity $\bar{N}N$ band. The model of Ref. 5 was used. The square of the corresponding radial wave function $b(r)$ is plotted as a dashed line. The meson-exchange produce a deep pocket of attraction at intermediate distances r, while the centrifugal term produces a repulsive barrier for both small and large r. The wave function is sharply localized in the region of strong attraction.

V. DISCUSSION

Since the early work of Fermi and Yang[17] on the pion as an $\bar{N}N$ composite, several qualitative comparisons between $\bar{N}N$ bound states and some part of the observed meson spectrum have been made.[1-4] Several years ago, the bootstrap hypothesis[18] rekindled interest in this type of speculation.

Recently, new motivations for studying the $\bar{N}N$ spectrum have emerged, since several models predict the existence of heavy mesons (for instance, multiquark states,[19] notably $qq\bar{q}\bar{q}$). As pointed out earlier on the basis of duality arguments,[20] some of these mesons are predominantly coupled to baryon-antibaryon configurations. However, from the quantitative viewpoint, the relation between the quark-model or S-matrix approach to the mesonic spectrum and potential calculations remains imprecise. For example, while the quark model takes account of the isospin degeneracy of Regge trajectories,[21] this property does not emerge automatically in the baryon-antibaryon spectrum. It is thus of particular interest to study the behavior of the $\bar{N}N$ system in this regard.

In the case of spin-singlet ($S=0$) states, the $\bar{N}N$ spectrum in some models consists of roughly de-

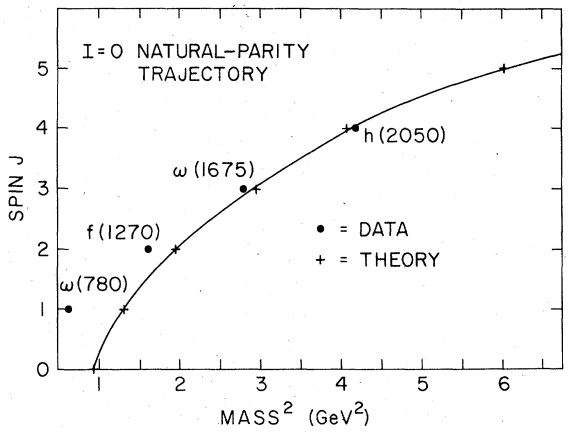

FIG. 5. Regge plot of the $I=0$ natural-parity meson trajectory. The experimentally observed $J^{PC}=1^{--}$, 2^{++}, 3^{--}, 4^{++} mesons (Ref. 24) are shown as black dots. The corresponding trajectory in the $\bar{N}N$ potential model ($^{13}S_1$-$^{13}D_1$, etc.) is displayed as a series of crosses. The model of Ref. 5 was used, with a cutoff radius of 0.75 fm. Note that the $\bar{N}N$ trajectory grazes the experimental one in the region of high spin ($3^-, 4^+$) near the $\bar{N}N$ threshold. A wide spin-5 resonance is predicted near 2.4 GeV.

generate doublets of $I=0$ and 1 states, because the isovector exchange potential V^- is relatively weak compared to the isoscalar potential V^+. An application of this idea has recently been proposed in Ref. 22 as a possible explanation of the behavior of $\bar{p}p$ cross sections in the vicinity of the structure[6,8] at 1932 MeV. This calculation is based on the model of Bryan and Phillips,[12] and contains a contribution from ρ exchange with a smaller coupling constant than obtained from more recent evaluations.[23] Also, in most of the more recent models of nuclear forces,[5,16] the contributions of ω and ϵ exchange are smaller than in the model of Bryan and Phillips.[12] This tends to diminish somewhat the preponderance of isoscalar exchange forces in $S=0$ states.

In the $\bar{N}N$ states of natural parity ($S=1$, $L\neq J$), the breaking of $I=0$, 1 degeneracy is much more important. This is due to the *coherence* of tensor forces which occurs only for $I=0$. This effect appears already in the previously published $\bar{N}N$ spectra,[1,4] but is accentuated by the inclusion of off-diagonal tensor forces, as one can see from an inspection of Tables III and V. Thus it is clear that one could only achieve isospin degeneracy in such potential models by including a much larger configuration space of baryon-antibaryon and meson-meson configurations.

We have seen how the presence of strong tensor forces favors the formation of a band of $\bar{N}N$ states with $I=0$, and $J^{PC}=0^{++}$, 1^{--}, 2^{++}, 3^{--}, 4^{++}, 5^{--}, etc. A Regge plot of J vs M^2 is shown in Fig. 5 for this band, in the case of the Paris potential with a cutoff $r_0=0.75$ fm, along with the corresponding experimentally observed mesons with the same quantum numbers. The experimental trajectory is approximately linear in M^2, while the potential model yields roughly $J\sim M$ [the relation $M_J\approx 766+317J$ (MeV) describes the theoretical results for $J\geq 1$]. It is noteworthy that the $\bar{N}N$ band passes near the experimental states in the region of the $\bar{N}N$ threshold; one might thus expect that the 3^- [$\omega(1675)$] and 4^+ [$h(2040)$] members might contain some admixture of the $\bar{N}N$ configuration. An additional high-spin meson (5^-) is predicted to lie around 2430 MeV; this is the coupled $^{13}G_5$-$^{13}I_5$ $\bar{N}N$ configuration. This energy is close to the U region,[24] where structure in the $\bar{p}p$ total cross section is seen.[25] A recent analysis[26] of the $\bar{p}p\to\pi^+\pi^-$ reaction in this energy region suggests wide 4^+ and 5^- resonances near 2400 and 2360 MeV, respectively. The 5^- resonance,[26] however, has isospin one rather than zero. It would be interesting to analyze data on channels which select $I=0$, such as $\bar{p}p\to\eta^0\eta^0$, with the assumption of a wide $J^{PC}(I^G)=5^{--}(0^-)$ resonance as predicted here. This structure should of course be absent in $\bar{p}p\to\pi^0\eta^0$, which selects $I=1$ states.

For the deeply bound low-spin members of the band shown in Fig. 5, radial excitations with $n=1$ are also predicted to be bound ($^{13}P_0$ and $^{13}S_1$-$^{13}D_1$ states in Table V). While it is premature to attempt any detailed comparison with experiment, the $n=1$ $^{13}S_1$-$^{13}D_1$ state could constitute some component of the 1^{--} meson recently discovered at the 1821 MeV.[27] In the usual quark model ($q\bar{q}$), this meson is also thought to be a radial excitation.[27] The $n=0$ $^{33}S_1$-$^{33}D_1$ state of Table V could have some overlap with the $\rho'(1600)$ meson of the same quantum numbers.[24]

We emphasize that the dynamical mechanism for producing *high-spin* (4^+ and 5^-) states in the $\bar{N}N$ model is the attractive *coherence* of tensor forces for $I=0$. The off-diagonal tensor force produces virtually complete mixing of orbital states with $L=J\pm 1$, and is particularly important in bringing the high-spin states down to energies not far from the $\bar{N}N$ threshold in some models. In the $\bar{N}N$ potential model, there is no coherence of the forces in $I=1$ states, so the $^{33}P_0$ (δ), $^{33}S_1+{}^{33}D_1$ (ρ), $^{33}P_2+{}^{33}F_2$ (A_2), etc., configurations lie much higher in energy than the $I=0$ band. This gives a large breaking of isospin degeneracy for $S=1$ states.

The importance of tensor forces is familiar from the case of the deuteron. In most models, the diagonal part of the $^3S_1$ potential is *shallower* than the $^1S_0$ potential. However, the tensor coupling of

$^3S_1$ and $^3D_1$ gives an additional attraction which is strong enough to bind the deuteron by a few MeV, although the D-state admixture in the wave function remains small. For the $I=0$ $\bar{N}N$ system, the effect of tensor forces is qualitatively similar, but much more dramatic; the tensor coupling can produce hundreds of MeV of additional binding (see Fig. 3 and Tables III and V) and gives large mixing of orbital states [see Eq. (3.2)].

It would be interesting to extend this work in several ways. Firstly, one must estimate the effects of annihilation on the $\bar{N}N$ states near threshold. It may be possible to describe the observed "background" $\bar{N}N$ scattering (ratio and energy dependence of total elastic and reaction cross sections) without washing out all narrow structures near threshold (which occurs if we use the imaginary potential of Ref. 12). It is also important to estimate the degree of mixing of other baryon-antibaryon configurations into the $\bar{N}N$ states calculated here. This may provide a clue as to whether isospin degeneracy can be attained in this picture.

ACKNOWLEDGMENTS

We would like to thank G. E. Brown for many stimulating discussions and for the hospitality extended to one of us (J.M.R.) by the Nuclear Theory Group at Stony Brook. We have also benefitted from useful conversations with W. Buck and S. Kahana. The work of C.B.D. was supported by the Energy Research and Development Administration under Contract No. EY-76-C-02-0016. The work of J. M. R. was supported by the Energy Research and Development Administration under contract no. AT(11-1)-3001.

*Permanent address: Laboratoire de Physique Théorique des Particules Elémentaires, Tour 16, E1, 4 Place Jussieu, 75230 Paris Cedex 05, France.

[1]O. D. Dalkarov, V. B. Mandelzweig and I. S. Shapiro, Nucl. Phys. B21, 88 (1970); I. S. Shapiro, Usp. Fiz. Nauk 109, 431 (1973) [Sov. Phys.—Usp. 16, 173 (1973)]; L. N. Bogdanova, O. D. Dalkarov and I. S. Shapiro, Ann. Phys. (N.Y.) 84, 261 (1974).

[2]G. Schierholz and S. Wagner, Nucl. Phys. B32, 306 (1971); G. Schierholz, Nucl. Phys. B7. 483 (1968); B40, 335 (1972); Nuovo Cimento 16A, 187 (1973).

[3]D. C. Peaslee, Phys. Rev. D 9, 272 (1974).

[4]C. B. Dover, in *Proceedings of the Fourth International Symposium on $\bar{N}N$ Interactions, Syracuse, New York, 1975*, edited by T. E. Kalogeropoulos and K. C. Wali (Syracuse Univ., Syracuse, 1975), Vol. II, Chap. VIII, pp. 37–91; a more complete list of references to earlier work on the $\bar{N}N$ system may be found here.

[5]J. M. Richard, M. Lacombe, and R. Vinh Mau, Phys. Lett. 64B, 121 (1976); For a review of the Paris potential, see R. Vinh Mau, in *Mesons in Nuclei*, edited by M. Rho and D. H. Wilkinson (North-Holland, Amsterdam, 1978).

[6]A. S. Carroll *et al.*, Phys. Rev. Lett. 32, 247 (1974); T. E. Kalogeropoulos and G. S. Tzanakos, Phys. Rev. Lett. 34, 1047 (1975).

[7]L. Gray, P. Hagerty, and T. E. Kalogeropoulos, Phys. Rev. Lett. 26, 1491 (1971).

[8]V. Chaloupka *et al.*, Phys. Lett. 61B, 487 (1976).

[9]H. I. Miettinen, Rapporteur's talk, in *Proceedings of the Third European Symposium on Antinucleon-Nucleon Interactions*, edited by G. Ekspong and S. Nilsson (Pergamon, New York, 1976); also SLAC Report No. 1813, 1976 (unpublished); see also talk by G. F. Chew at this conference.

[10]G. F. Chew and C. Rosenzweig, Phys. Lett. B58, 93 (1975); Phys. Rev. D 12, 3907 (1975); Nucl. Phys. B104, 290 (1976).

[11]F. Myher and A. W. Thomas, Phys. Lett. 64B, 59 (1976); F. Myhrer and A. Gersten, Nuovo Cimento 37A, 21 (1977); I. Ulehla, Saclay report, 1976 (unpublished). O. D. Dalkarov and F. Myhrer, Nuovo Cimento 40A, 152 (1977); J. P. Elagin *et al.*, Phys. Lett. 7, 352 (1963); M. S. Spergel, Nuovo Cimento 47A, 410 (1967).

[12]R. A. Bryan and R. J. N. Phillips, Nucl. Phys. B5, 201 (1968).

[13]I. S. Shapiro, Phys. Rep. 35C, 129 (1978).

[14]H. P. Stapp *et al.*, Phys. Rev. 105, 302 (1957).

[15]J. M. Blatt and L. C. Biedenharn, Rev. Mod. Phys. 24, 258 (1952).

[16]See, for instance, G. E. Brown and A. D. Jackson, *The Nucleon-Nucleon Interaction* (North-Holland, Amsterdam, 1976), for a review of dispersion techniques applied to the NN system.

[17]E. Fermi and C. N. Yang, Phys. Rev. 76, 1739 (1949).

[18]See M. Jacob and G. F. Chew, *Strong Interaction Physics* (Benjamin, New York, 1964), Chap. 4.

[19]R. L. Jaffe, Phys. Rev. D 15, 267 (1977); 15, 281 (1977); these papers contain references to earlier work on the MIT bag model.

[20]J. Rosner, Phys. Rev. Lett. 21, 950 (1968); 22, 689 (1969); H. J. Lipkin, Nucl. Phys. B9, 349 (1969).

[21]For a discussion of degeneracy properties of Regge trajectories, see V. Barger and D. Cline, *Phenomenological Theories of High Energy Scattering* (Benjamin, New York, 1969).

[22]C. Dover and S. Kahana, Phys. Lett. 62B, 293 (1976).

[23]G. Höhler and E. Pietarinen, Nucl. Phys. B95, 210 (1975); P. Gauron, private communication.

[24]Particle Data Group, Rev. Mod. Phys. 48, S1 (1976); see p. S131.

[25]R. J. Abrams *et al.*, Phys. Rev. D 1, 1917 (1970).

[26]E. Eisenhandler *et al.*, Nucl. Phys. B96, 109 (1975); A. A. Carter *et al.*, in *Proceedings of the Third European Symposium on Antinucleon-Nucleon Interactions*, Stockholm, 1976, edited by G. Ekspong and S. Nilsson (Pergamon, New York, 1976); see also the Rapporteur talk by E. Eisenhandler at this conference for a review of data on $\bar{p}p \to \pi\pi$, $\pi\eta$ among other topics; A. A. Carter *et al.*, Phys. Lett. 67B, 117 (1977).

[27]C. Bacci *et al.*, Phys. Lett. 68B, 393 (1977); B. Esposito *et al.*, *ibid.* 68B, 389 (1977); G. Barbiellini *et al.*, *ibid.* 68B, 397 (1977).